# Effect of microbial transglutaminase on functional, rheological, and structural properties of lentil protein-casein binary gels

**Qi Tang[a,b], Yrjö H. Roos[b], Song Miao[a,c]***

[a] Teagasc Food Research Centre, Moorepark, Fermoy, Co. Cork, Ireland

[b] School of Food and Nutritional Sciences, University College Cork, Cork, Ireland

[c] China-Ireland International Cooperation Center for Food Material Science and Structure Design, Fujian Agriculture and Forestry University, Fuzhou, China

* Correspondence: song.miao@teagasc.ie; Tel.: +353-(0)-25-42468

**Abstract**

In recent years, various strategies have been introduced to partially substitute animal proteins with plant proteins. This study applied microbial transglutaminase (MTGase) to crosslink lentil protein isolate (LPI) and casein. The gel mixture prepared using different LPI-casein ratio (4:0, 3:1, 2:2, 1:3, 0:4), and the structural, gelation characteristics of these hetero-mixtures were investigated. SDS-PAGE showed the bands of vicilins (~ 50 kDa), and 11S acidic subunit (~ 40 kDa) almost disappeared and partly 11S basic subunit (20 kDa) involved in the polymerization, whereas almost all the bonds of casein were involved in the MTGase-induced gelation process. With the increasing concentration of casein, LPI-casein binary gels presented enhanced mechanical textural properties (increased from 284.83 to 1128.33g of hardness), rheological properties (increased from 105.8 to 4405 Pa of storage modulus), water holding capacity (increased from 63.86 to 98.82%) and more homogeneous and compact microstructural properties (CLSM, SEM) as a result of homologous and heterologous crosslinking mediated by MTGase. Interestingly, gels prepared by partial casein replacement (by 25% LPI) had similar textural, water holding capacity, and microstructural properties to those prepared by casein-alone gels, demonstrating the possibility of successfully replacing casein with 25% LPI in MTGase induced system. This study presents a new interaction strategy mediated by MTGase for LPI and casein binary system to greatly enhance their gelation performance, as well as the potential of LPI in substitute dairy to formulate diversified food products.

**Keywords:** lentil protein, casein, MTGase, binary gel, gelation property

## 1. Introduction

Proteins are an indispensable part of human nutrition because of their role in muscle protein synthesis, immune response, and metabolic regulation (Shevkani & Chourasia, 2021). Casein micelles, for instance, is a commonly used ingredient in food products, represent about 80% of the total protein in milk (Huppertz, Fox, & Kelly, 2018). It is composed of four phosphorylated proteins: $\alpha_{S1}$-, $\alpha_{S2}$-, β- and κ-caseins, and these proteins are rheomorphic and poorly defined tertiary structures (Lin, et al., 2019). Nevertheless, there is a surging trend to replace animal-based proteins (such as dairy protein) with plant proteins due to sustainability, cost, and environmental concerns (Aschemann-Witzel, Gantriis, Fraga, & Perez-Cueto, 2021; Zhu, Huang, Guo, & Chen, 2021). Protein from lentils (*Lens culinaris L.*) is high-quality, health-promoting, but underutilized (Steinfeld, et al., 2015). It is mainly composed of globulins (~70 % of total protein), which consist of legumin-like (11S, ~50 %) and vicilin-like (7S) group fractions. Exploring different technological routes to design food products containing binary plant and dairy proteins is a strategy to meet the increasing demand for versatile protein sources. This will also allow utilization of any synergistic functional effects that might occur in plant and dairy protein systems (Kornet, et al., 2021).

Gelation properties are important to the textural and sensory perception of many food products, including yogurt, cheese, eggs, and meat (Kornet, et al., 2021; McClements & Grossmann, 2021). Generally, two different methods are employed to produce gels: heat-induced gels (heating) and cold-induced gels (salts, acids, enzymes) (Alves & Tavares, 2019). However, developing a hybrid gel system composed of plant and dairy protein mixture is challenging due to the significant differences between their composition, structural, and functional properties (Alonso-Miravalles, et al., 2019; Kornet, et al., 2021; Wu, et al., 2020). For instance, Beliciu and Moraru (2011) reported

phase separation of casein and soy proteins mixtures after heat treatment, with their rheological properties mimicking those of soy protein other than casein. Mession, Roustel, and Saurel (2017) found that although casein altered the heat-induced interactions between pea proteins in the mixed systems, casein was not involved with the pea protein. It is worthy to consider that casein possesses excellent thermal stability, which can withstand temperatures up to at least 90 ℃ in milk, and do not form gels when heated below 100 ℃ at pH 6.8 (Beliciu & Moraru, 2013; Nicolai & Chassenieux, 2021; O'connell & Fox, 2003).

Interestingly, microbial transglutaminase (MTGase; EC 2.3.2.13) is a safe and effective enzyme that generates ε-(γ-glutamyl)-lysine (Gln-Lys) isopeptide bonds by cross-linking inter- and intra-molecular reactions between Lys-ε-amino and Gln-γ-amide groups of proteins (Qin, et al., 2016). Unlike heat induced gels, this enzyme help forms rigid and resistant gel networks due to the association of protein molecules by isopeptide bonds, which approximately 20-fold stronger than non-covalent bonds (Liu, et al., 2020). Hence, it offers the great potential of providing desired gel performance for diversified market demands in relatively mild conditions. Recently, a growing number of studies have been conducted to modify the gelation properties of signal protein system using MTGase alone or in combination with other techniques (enzymatic hydrolysis and ultrasound, etc.) (Djoullah, Husson, & Saurel., 2018; Gao, et al., 2021; Ma, et al., 2022; Raak & Corredig, 2022). These studies demonstrated that MTGase-induced gel performance varied with different protein substrates due to the quantity of Gln and Lys residues as well as the accessibility of TGase to these two reactive groups (Djoullah, et al., 2018). For instance, it was reported that MTGase can significantly improve the gelling properties of legume proteins (e.g. SPI) and legumin acidic subunits are more easily cross-linked than legumin basic subunits in legume

proteins (Zheng, Regenstein, Zhou, & Wang, 2022). Casein has been reported to be easily crosslinked by MTGase, with susceptibility to MTGase polymerization descending in the order $\kappa > \beta > \alpha_{S1} > \alpha_{S2}$ in skim milk (Duerasch, Wissel, & Henle, 2018; Raak, et al., 2022). Nevertheless, no systematic study has been conducted to date on the gelation performance of MTGase-induced lentil protein and casein binary systems.

Therefore, the novelty of this study is to develop a new interaction strategy of binary protein systems between LPI and casein mediated by MTGase to achieve desired gelation performance, as well as exploring the potential of plant protein to formulate diversified food products with alternative dairy proteins. It was hypothesized the lentil protein isolate-casein binary systems treatment by MTGase would resulted in improved gel performance, and LPI would show potential in replacement of dairy protein in formatting diversified products. This hypothesis was validated by investigating the structural, rheological, and mechanical properties of LPI-casein binary gels at different ratios.

## 2. Material and methods

### 2.1. Materials

Lentil protein isolate (LPI) was kindly provided by Fraunhofer (Munich, Germany) having a protein purity 83.36 % ± 3.86 (dry basis). Casein micelles (80.58 % ± 1.40 protein on dry basis) was purchased from VWR (Leicestershire, England). A $Ca^{2+}$ independent microbial transglutaminase (MTGase, Batch No: 2021089-100) derived from bacterium *Streptomyces Mobaraensis* was kindly provided by Stabizym GmbH (Roßdorf, Germany) with a declared activity of 100-120 U/g. All chemicals were of analytical grade.

## 2.2. Preparation of MTGase-induced LPI-casein gels

The protein solutions (14 %, *w/w*) were prepared by dissolving LPI and casein protein powders in deionized water, respectively, and then stirred overnight at ambient temperature. The obtained solutions were mixed in the LPI to casein ratio of 4:0, 3:1, 2:2, 1:3, and 0:4 and were named as L4C0, L3C1, L2C2, L1C3, L0C4, respectively. The obtained solutions were adjusted to pH 7.5 using sodium hydroxide under continuous stirring for 40 min. Afterwards, the protein solutions with the addition of MTGase (15 U/g protein) were incubated at water bath (50 ℃) for 2 h. The obtained gels were then immediately cooled using an ice bath to stop the reaction and stored at 4 ℃ for further analyses.

## 2.3. SDS-PAGE analysis

SDS-PAGE was used to analyze the LPI-casein mixtures and gels under reducing (dithiothreitol, DTT) and non-reducing conditions. Protein sample (1 μL) was mixed with 30 μL LDS sample buffer (4X, Invitrogen, Thermo Fisher Scientific, Cork, Ireland) and 3 μL reducing agent (10X, Invitrogen, Thermo Fisher Scientific, Cork, Ireland) and placed in water bath at 70 ℃ for 10 min. After cooling to room temperature, the sample was centrifuged at 5000× *g* for 10 min at 4 ℃. Next, the obtained sample (10 μL) and PageRuler unstained protein ladder (10 μL) (Thermo Fisher Scientific Inc., Cork, Ireland) were injected into a commercial polyacrylamide gel, separately. SDS-PAGE analysis was conducted with 12% Mini-PROTEAN® TGX™ Precast protein gels (Bio-Rad Laboratories, Dublin, Ireland) and was performed at 200 V for 30 min using a Mini-PROTEAN Tetra System (Bio-Rad Laboratories, Dublin, Ireland). After electrophoresis, the gels were stained with Coomassie Blue R-250 for 2 h and destained overnight. The gels were then scanned with an Epson perfection V850 Pro scanner.

## 2.4. Least gelling concentration

The least gelling concentration (LGC) of LPI-casein admixtures was studied by preparing concentrations of protein solutions from 2 to 20% (*w/w*) at pH 7.5 (Djoullah, Djemaoune, Husson, & Saurel, 2015). MTGase (15 U/g protein) was added into protein solutions and heated in water bath (50 ℃) for 2 h, and then immediately cooled down in ice bath. The samples were stored at 4 ℃ for 24 h before analysis. The lowest gelling concentration at which samples did not flow when tubes were inverted was deemed as LGC.

## 2.5. Dynamic oscillation analysis

### 2.5.1. Time Sweep Measurements

The dynamic oscillation analysis (time sweep and frequency sweep) of LPI-casein mixtures of different ratios (4:0, 3:1, 2:2, 1:3, 0:4) were performed using an AR2000ex rheometer (TA Instruments Ltd., Crawley, UK). Rheological measurements were carried out with a gap distance of 5920 μm, which is specific gap recommended for concentric cylinder geometry by the rheometer supplier. The temperature of the bottom plate was controlled using a peltier system (Viscotherm VT2, Phar Physica, Netherlands). In order to prevent evaporation of moisture during the test, the sample was sealed by paraffin oil. After adding MTGase (15 U/g protein) to protein solutions (14 %, w/w), the solutions (20 mL) were mixed and then poured into the concentric cylinder geometry (50 ℃) before performing test. Gelation conditions were the same as those described in Section 2.2. The time sweep measurement was performed by incubating samples at 50 ℃ with a frequency of 1 Hz and strain of 0.04 % (within the linear viscoelastic region).

### 2.5.2. Frequency Sweep measurements

Frequency sweep analysis was carried out within linear viscoelastic region over a frequency range of 0.01 to 100 Hz at a fixed strain of 0.04% (50 ℃).

## 2.6. Texture analysis

The texture attributes of the gels were evaluated using a Texture Analyzer TA-XTplus/30 (Stable Microsystem, Surrey, UK). The MTGase-induced LPI-casein gels were prepared as described above with slight modifications. Briefly, the prepared solutions were poured into 120 mL scaled cylinders (diameter- 40 mm). Afterwards, MTGase was added and incubated at 50 ℃ for 2h. The gels were stored at 4 ℃ for overnight and the column shaped gels were carefully taken out and cut into cylinders (40 mm × 25 mm) for texture analysis. The gels were tested at room temperature (~ 20 ℃) using a two-bite compression test with a SMS P/75R probe at a test speed of 1 mm/s, trigger force of 5 g and deformation of 40 %. Hardness, cohesiveness, springiness and gumminess were calculated by the software Texture Exponent (Stable Micro Systems).

## 2.7. Water holding capacity (WHC)

The water holding capacity (WHC) of prepared gels were determined according to the method of Li, et al. (2018) with slight modifications. Briefly, a total of 10 g LPI-casein mixed solutions (14% *w/w*, pH 7.5) and MTGase (15 U/g protein) were poured in a 15 mL centrifuge tube. The samples were thoroughly mixed and incubated at 50 ℃ for 2 h. Thereafter, gels were immediately cooled and stored at 4 ℃ for 24 h. The gels ($M_G$) were centrifuged at 8000× *g* for 10 min at 20 ℃. The mass of expelled water ($M_W$) was collected and the weight was recorded. The WHC was calculated:

176 $$WHC\ (\%) = \left(\frac{M_G - M_W}{M_G}\right) \times 100 \qquad (1)$$

177 **2.8. Confocal laser scanning microscopy (CLSM)**

178 A confocal scanning laser microscope (Leica Microsystems CMS GmbH, Germany)
179 fitted with an inverted camera and equipped with 63X lens was used in this study
180 (Pereira, Bennett, Hemar, & Campanella, 2001). To stain the protein phase of the gels,
181 Rhodamine B powder (0.1 g) was dissolved in 100 mL Milli Q water. The sliced
182 MTGase-induced LPI-casein gels were transferred to a glass slide, stained with dye
183 solution, and covered with a cover slip. When 63X lens was used, an oil drop was added
184 over the cover slip. Rhodamine B dye was excited at 559 nm and the emission band
185 was collected at 590-640 nm. Rhodamine dye was excited using a He-Ne laser with an
186 excitation line of 488 nm.

187 **2.9. Scanning electron microscopy (SEM)**

188 Scanning electron microscopy was used to observe changes in the microstructure of
189 gels as per the methodology of Deshwal, et al. (2020). Gels were sliced into cube sample
190 and fixed in 2.5% glutaraldehyde in a 0.05 M sodium phosphate buffer for 3 h at room
191 temperature. Fixed samples were dehydrated in graded ethanol ranging from 50 to 100%
192 for 15 minutes. Samples were rapidly frozen and dried. The dried samples were
193 mounted on an aluminium stun and coated with gold. The microstructure was observed
194 using a scanning electron microscope (SEM-Zeiss Supra 40VP filed emission, Carl
195 Zeiss AG, Darmstadt, Germany) at an accelerating voltage of 10 kV and representative
196 images were captured.

### 2.10. Statistical analysis

All measurements were performed three times and were reported as mean ± standard deviation. One-way ANOVA analysis was performed using SPSS 20.0 software (Chicago, USA) and significant differences between groups was determined by the Duncan's test at 5% level of significance ($p < 0.05$).

## 3. Results and discussion

### 3.1. MTGase-induced LPI-casein gel formation

Our preliminary experiments showed that LPI and casein mixtures did not form gel without MTGase addition (50 ℃), whereas all LPI and casein mixtures formed self-supporting gels on the addition of MTG (15 U/g protein) (Fig. 1a-b). It is worthy to consider that casein possesses excellent thermal stability, which can withstand temperatures up to at least 90 ℃ in normal milk pH and ionic conditions, and do not form gels when heated below 100 ℃ at pH 6.8 (Beliciu, et al., 2013; Nicolai, et al., 2021). Furthermore, LPI denatures at roughly 100 ℃ at neutral pH (Ladjal-Ettoumi, Boudries, Chibane, & Romero, 2016). The high denaturation temperature of LPI and casein might explain why there were no gels formed at 50 ℃. It can be therefore demonstrated that the formed gels under these experiment conditions were induced by MTGase rather than heating (50 ℃). Moreover, Djoullah, et al. (2018) also reported that transglutaminase catalyzed cross-linking reactions other than heating led to the formation of pea globular gels when treated with MTGase (incubated at 40 °C). Gel formation can be influenced by pH, protein concentration, molecular weight, and interactions between proteins (Raikos, Campbell, & Euston, 2007). Hydrophilic bonds, hydrogen bonds and disulfide bridges are the main forces involved in stabilizing heat-

induced gels (Sun & Arntfield, 2012). The formed MTGase-mediated isopeptide bond (G-L), however, help improve protein-protein interactions during gel formation, and are more powerful than hydrogen bonds and hydrophobic bonds (Alves, et al., 2019; Dube, Schäfer, Neidhart, & Carle, 2007; Tang, et al., 2006).

### 3.2. SDS-PAGE analysis

Non-reducing (NR) (Fig. 2a, c) and reducing SDS-PAGE (R) (Fig. 2b, d) analysis were used to investigate the interactions between LPI and casein without/with MTGase treatment. Fig. 2a-b shows the bands related to LPI and casein protein fractions without MTGase treatment (50 ℃). L4C0 showed intense bands in the range of 45-55 kDa, while L0C4 showed complete absence of these bands (Fig. 2a). Globulins and albumins are the two major components in LPI, and the major globulins in LPI are legumin-rich fractions (~60 kDa) and vicilin-rich fractions (~50 kDa) (Baugreet, et al., 2019; Tang, Roos, & Miao, 2023). Among them, the legumin-rich fraction comprises acidic (~40 kDa) and basic (~20 kDa) subunits linked by disulfide bridges, which were therefore more intense in reducing conditions (Fig. 2b). For LPI-casein admixed samples, the most intense bonds (~50 kDa) are probably vicilin, which is an oligomeric protein composed of three polypeptide subunits (α, β and γ) (Ladjal-Ettoumi, et al., 2016). Samples having only casein protein (L0C4) showed very strong bands at 25-35 kDa indicating individual casein protein fractions αs1-, αs2-, β-, and κ-casein (Ghosh, Ali, & Dias, 2009). On the other hand, these casein bonds were less intense in LPI-casein admixed samples.

Most protein bands disappeared after MTGase treatment, suggesting successful intra/inter-molecularly linkages between protein fractions, resulting the formation of complexes with high molecular weights which were unable to penetrate resolving gels

(Fig. 2c-d). Zhou, Zheng, Zhong, Wang, and Deng (2022) reported a similar result on hempseed protein-casein that MTGase treatment caused high molecular polymer formation by cross-linking between protein fractions. With decrease in ratio of LPI to casein, the bands of vicilins (~50 kDa) and 11S acidic subunit (~40 kDa) almost disappeared, indicating involvement of these bands in LPI-casein complexes. Fig. 2c-d showed faded bands of 11S basic subunit (20 kDa) in LPI-containing sample probably as a result of LPI involvement in polymerization. These results were similarly reported in previous studies (Djoullah, et al., 2015; Larre, Chiarello, Dudek, Chenu, & Gueguen, 1993; Larre, Kedzior, Chenu, Viroben, & Gueguen, 1992). It might be attributed to the hypothesize that the majority of the legumin acidic subunits are found on the surface, while the basic subunits are located inside the hydrophobic core of the protein (Djoullah, et al., 2015; Gueguen, Chevalier, And, & Schaeffer, 1988). The non-disappearance of bands in LPI-containing samples could be an indication that MTGase had difficulty accessing glutamine and lysine residues during the cross-linking reaction due to the compact structure of globular proteins in LPI (DeJong & Koppelman, 2002; Zha, Rao, & Chen, 2021). It is noteworthy that there was no significant difference in non-reducing and reducing electrophoretic patterns for LPI-casein mixtures with MTGase treatment (Fig. 2c-d). This demonstrated that ε-(γ-glutamyl)-lysine (Gln-Lys) isopeptide bonds generated by MTGase that are unbreakable via DTT and SDS are the major driving force for high molecular polymers formation.

In contrast, the bonds of 25-35 kDa in casein-containing samples disappeared after MTG treatment, demonstrating that almost all casein fractions (κ, β, $\alpha_{S1}$, $\alpha_{S2}$) were involved in complexation, which confirmed the previous findings (Raak, et al., 2022). This might be explained by the more flexible structures of casein and its high Gln and Lys residues content (Duerasch, et al., 2018; Holt & Sawyer, 1993).

### 3.3. Least gelling concentration

A three-dimensional network of proteins can be induced if the protein concentration is sufficiently high and stabilized by protein interactions (covalent and/or noncovalent); otherwise protein aggregates form (Alves, et al., 2019). The least gelation concentration (LGC), is commonly used parameter for measuring gelling capacity, with a higher value of LGC indicating lower gelling capacity (Moure, Sineiro, Domínguez, & Parajó, 2006). It is notable that the LGC varied with the different ratios of LPI and casein. For instance, compared to samples with a low casein concentration (L4C0, L3C1, and L2C2), samples with high casein concentrations (L3C1, L4C0) showed lower LGC (10 %), exhibiting greater gelling abilities (Table 1). As can be observed in section 3.2, almost all casein fractions can be used for MTGase cross-linking during gel formation, whereas the protein fractions in LPI can only be partially cross-linked due to its compact globular structure (Duerasch, et al., 2018). Consequently, a higher level of covalent isopeptide bonds can be formed between casein and LPI fractions for high casein-containing samples, contributing to a higher gelling capacity and lower LGC. To our knowledge, there is no study to compare the LGC in the LPI-casein system induced by MTGase.

### 3.4. Rheological properties

Time sweep analysis were conducted to monitor the gelation kinetics of MTGase-induced gelation process of LPI-casein binary systems at different ratios (4:0, 3:1, 2:2, 1:3, 0:4) and presented in Fig. 3a-b. Storage modulus (G′) and loss modulus (G″) which represent the elastic/solid and viscous/liquid properties of samples, respectively, were recorded during this process. Loss tangent (tan δ) reflects the boundary of sol-gel transition by the cross-over of the G′ and G″ at the gel point where tan $\delta = G''/G' = 1$,

indicating that samples pass from a preponderantly viscous/liquid state (tan $\delta > 1$) to an elastic/solid dominate state (tan $\delta \leq 1$) (Djoullah, et al., 2018; Li, Guo, Yang, & Guo, 2022). In the beginning, all mixed systems showed liquid-like behaviors, as G″ > G′ (Fig. 3a-b). Then the storage modulus (G′) and loss modulus (G″) of all protein samples exhibited a rapidly rise, suggesting start of gel network formation ($t < 2000$ s). Afterward, the G′ and G″ values for all samples gradually levelled off and reached a plateau with G′ > G″ and tan $\delta < 1$, which indicated that all the samples showed preponderantly elastic/solid like properties regardless of the LPI-casein ratio.

The lowest G′ and G″ was found in L4C0 (G′ =105.80 Pa, G″= 54.20 Pa) at the end of gelation (t = 14000 s). This could be explained that the limited number of Gln and Lys residues in LPI as well as its tight globular structure make accessing these reactive groups difficult for TGase, resulting in fewer Gln-Lys isopeptide bonds being formed and poor rheological properties (DeJong & Koppelman, 2002; Zha, Rao, & Chen, 2021). With the decreasing ratio of LPI to casein, the highest G′ was found in L0C4 (4405 Pa), followed by L1C3 (1675.6 Pa), and L2C2 (441.4 Pa). It is estimated that these gels have significantly improved rheological properties since more Gln-Lys isopeptide bonds are generated by MTGase at higher ratios of casein, resulting in a more uniform and denser three-dimensional gel network (Qin, et al., 2016). The results were in accordance with the electrophoretic patterns shown in Fig. 2c-d and LGC (Table 1), in which the enhanced protein cross-linking resulted in better gel performance at high ratios of casein.

The network structure of MTGase-induced LPI-casein binary gels were investigated as a function of frequency (0.01-100 Hz). This further confirmed that 3D gel networks with solid dominate behavior were formed, as all samples had considerably higher G′ than G″ (Fig. 3c-d). Moreover, with increasing percentage of casein, G′ of mixed LPI-

casein gel system increased, indicating a higher casein content increased gel strength of LPI-casein gel system effectively.

### 3.5. Texture and water holding capacity

The mechanical properties (hardness, springiness, cohesiveness, gumminess, and resilience) of MTGase-induced gel systems based on the different ratios of LPI and casein are shown in Table 2. Hardness is determined by the force required to compress the gel between dentition (solid state) or tongue and palate (semi solid state), and it relates to strength of the gel structure under compression (Yuan, Xu, Cui, & Wang, 2019). In this study, the increase in the mechanical properties was significantly ($p < 0.05$) observed with the increasing ratio of casein. For example, the hardness of the gels in L3C1 (415.87 g), L2C2 (585.41 g), L1C3 (1024.09 g), L0C4 (1128.33 g) was 1.46, 2.06, 3.60, 3.96 times higher than that in L4C0 (284.83 g), respectively. This is consistent with the results for the electrophoretic patterns (Fig. 2) and rheological properties (Fig. 3) of the LPI-casein gels, highlighting the possibility that higher casein ratios may result in more ε-(γ-glutamyl)-lysine cross-linking, which would improve gel strength. In addition, cohesiveness, as well as springiness, gumminess, and resilience tend to increase with the increasing proportion of casein. However, L1C3 and L0C4 did not differ significantly in textural properties (springiness, cohesiveness, resilience), and the hardness of L0C4 was only1.10-fold higher than that in L1C3. It can be assumed that the binary gels prepared by partial replacement of casein with 25% LPI could present similar mechanical properties as casein-alone through MTGase-induced reaction.

The WHC of a gel refers to the amount of water retained within the gel under enforced conditions, which is affected by stiffness and pore size of the gel network (Khalesi, Sun,

He, Lu, & Fang, 2021; Yang, Ren, Liu, Huo, & Li, 2021). As was shown in Table 2, the highest WHC was found in L3C1 (98.96 %), followed by L0C4 (98.82 %), L2C2 (86.01 %), L3C1 (79.68 %), and L4C0 (63.86 %), respectively. With increasing casein content, WHC of gels increased, reflecting a harder, denser, and more compact structure. This could be attributed to formation of more chemical bonds between proteins, and creation of more homogenous 3D network with higher ability to trap more water within the network (Peng & Guo, 2015; Yang, et al., 2021). Interestingly, there was no significant difference between the WHC of L3C1 and L0C4 ($p < 0.05$), and they approached an asymptotic maximum value of approximately 99%, demonstrating almost all water can be trapped within its network structure. This result was in line with the findings of textural analysis, indicating that replacement of casein up to 25% LPI could provide comparable WHC to casein-alone.

### 3.6. Appearance and microstructure

The gel structure can affect its textural, rheological, and functional properties. Fig. 4 shows the visual appearance (a-e), confocal microscopy (f-j) and SEM images (k-o) of LPI-casein gels. The visual images (Fig. 4a-e) show that all the gels were self-supporting, indicating that MTGase can induce uniform appearance of LPI-casein binary gels regardless of their proportions. This result was in accordance with the findings shown in Table 1. Furthermore, the gels became stiffer with increasing casein ratio as observed visually.

The Fig. 4f-j shows the CLSM images of gel samples wherein, red color indicates protein bodies. The microstructure of gels with L4C0, L3C1 and L2C2 were micrometer-sized particulate gel structures with irregular-shaped protein aggregates. The random shapes and sizes of aggregates can be explained by cross-linking of protein

fractions during MTGase-induced gel formation. It is interesting to note that L1C3 and L0C4 were homogeneous showing more uniform networks than the gel samples with higher casein ratios. This suggested that the substitution of casein by 25% LPI could develop a homogenous network structure as casein-alone.

SEM analysis was carried out to gain a more detailed understanding of gel structures of MTGase-induced LPI-casein gels at different ratios (Fig. 4k-o). As expected, the gels at relatively low casein concentrations (e.g. L4C0, L3C1 and L2C2) showed coarse structure with sheet-like aggregates. On the contrary, by increasing the casein ratio to 75% (*w/w*, L1C3) and 100% (*w/w*, L0C4), the gel structure became more homogeneous, compact, and had extremely small pores, suggesting a higher cross-linking density. These results were consistent with previously results (e.g. rheological, textural, WHC, and CLSM analysis), and confirmed that the variation in concentration of lentil to casein led a significant difference in gel structure. Consequently, partial replacement of casein (25% with lentil) yielded the orderly, fine gel structure, along with high gel strength, and thereby supported the great potential for LPI as a food substitute for dairy protein.

## 4. Conclusions

The characteristics of LPI-casein gel induced by MTGase were investigated at different ratio of concentrations (4:0, 3:1, 2:2, 1:3, 0:4). MTGase can induce self-standing LPI-casein binary gels regardless of their proportions, whereas the ratio of lentil to casein significantly altered their rheological, textural and microstructural properties. The electrophoretic patterns showed that almost all casein fractions, 11S acidic subunit (40 kDa) and 7S vicilins (50 kDa) of LPI were cross-linked with MTGase treatment, while the 11S basic subunit (20 kDa) of LPI only partially cross-linked during gel formation. The WHC, mechanical and rheological (G′) properties increased with decreasing ratio

of LPI to casein. Moreover, a partial replacement of casein with 25% LPI can result in binary gels with comparable mechanical properties (1024.09 and 1128.33g of hardness), WHC (98.96 and 98.82%), and fine microstructural properties to casein-alone. Partial replacement of LPI by casein can also considerably increase its gelation performance as compared to LPI-alone. The results of the current study could be beneficial to formulate food products with alternative dairy protein such as lentil. Therefore, this study demonstrated that binary LPI-casein systems mediated by MTGase can effectively improve gel performance and supported great potential of LPI for diversified food product formulation with alternative dairy proteins. Further study is required to evaluate the role and mechanism of protein fractions of LPI (vicilins, 11S acidic subunit, 11S basic subunits, α, β and γ- vicilin, convicilin) and casein ($\alpha_{S1}$-, $\alpha_{S2}$-, κ- and β- casein) in formation of intra/intermolecular bonds within MTG-induced gel network. Moreover, it is important to investigate how MTGase regulates the gelling mechanism of LPI-casein binary gels in real food system. For industrial applications, further study can be conducted to design desirable binary LPI and casein gelation properties under optimum MTGase addition and reaction conditions.

## CRediT author contribution statement

Qi Tang: Conceptualization, Methodology, Writing - original draft, Data curation, Investigation. Yrjö H. Roos: Supervision, Writing - review & editing. Song Miao: Supervision, Conceptualization, Writing - review & editing, Funding acquisition, Project administration.

## Declaration of competing interest

The authors declare that they have no known competing financial interests or personal relationships that could have appeared to influence the work reported in this paper.

## Acknowledgement

This work was supported by the China Scholarship Council (No. 201908320414) and Horizon 2020 European Union funded research innovation programme SMART PROTEIN Project (No: 862957).

## References

Alonso-Miravalles, L., Jeske, S., Bez, J., Detzel, A., Busch, M., Krueger, M., Wriessnegger, C. L., O'Mahony, J. A., Zannini, E., & Arendt, E. K. (2019). Membrane filtration and isoelectric precipitation technological approaches for the preparation of novel, functional and sustainable protein isolate from lentils. *European Food Research and Technology, 245*(9), 1855-1869. http://doi.org/10.1007/s00217-019-03296-y.

Alves, A. C., & Tavares, G. M. (2019). Mixing animal and plant proteins: Is this a way to improve protein techno-functionalities? *Food hydrocolloids, 97*, 105171. http://doi.org/10.1016/j.foodhyd.2019.06.016.

Aschemann-Witzel, J., Gantriis, R. F., Fraga, P., & Perez-Cueto, F. J. (2021). Plant-based food and protein trend from a business perspective: markets, consumers, and the challenges and opportunities in the future. *Critical Reviews in Food Science and Nutrition, 61*(18), 3119-3128. http://doi.org/10.1080/10408398.2020.1793730.

Baugreet, S., Gomez, C., Auty, M. A., Kerry, J. P., Hamill, R. M., & Brodkorb, A. (2019). In vitro digestion of protein-enriched restructured beef steaks with pea protein isolate, rice protein and lentil flour following sous vide processing. *Innovative food science & emerging technologies, 54*, 152-161. http://doi.org/10.1016/j.ifset.2019.04.005

Beliciu, C. M., & Moraru, C. I. (2011). The effect of protein concentration and heat treatment temperature on micellar casein–soy protein mixtures. *Food hydrocolloids, 25*(6), 1448-1460. http://doi.org/10.1016/j.foodhyd.2011.01.011.

Beliciu, C. M., & Moraru, C. I. (2013). Physico-chemical changes in heat treated micellar casein–Soy protein mixtures. *LWT-Food Science and Technology, 54*(2), 469-476. http://doi.org/10.1016/j.lwt.2013.06.013.

DeJong, G., & Koppelman, S. (2002). Transglutaminase catalyzed reactions: impact on food applications. *Journal of food science, 67*(8), 2798-2806. http://doi.org/10.1111/j.1365-2621.2002.tb08819.x.

Deshwal, G. K., Ameta, R., Sharma, H., Singh, A. K., Panjagari, N. R., & Baria, B. (2020). Effect of ultrafiltration and fat content on chemical, functional, textural and sensory characteristics of goat milk-based Halloumi type cheese. *LWT, 126*, 109341. http://doi.org/**10.1016/j.lwt.2020.109341**.

Djoullah, Husson, & Saurel. (2018). Gelation behaviors of denaturated pea albumin and globulin fractions during transglutaminase treatment. *Food hydrocolloids, 77*, 636-645. http://doi.org/10.1016/j.foodhyd.2017.11.005.

Djoullah, A., Djemaoune, Y., Husson, F., & Saurel, R. (2015). Native-state pea albumin and globulin behavior upon transglutaminase treatment. *Process Biochemistry, 50*(8), 1284-1292. http://doi.org/**10.1016/j.procbio.2015.04.021**.

Dube, M., Schäfer, C., Neidhart, S., & Carle, R. (2007). Texturisation and modification of vegetable proteins for food applications using microbial transglutaminase. *European Food Research and Technology, 225*(2), 287-299. http://doi.org/**10.1007/s00217-006-0401-2**.

Duerasch, A., Wissel, J., & Henle, T. (2018). Reassembling of alkali-treated casein micelles by microbial transglutaminase. *Journal of agricultural and food chemistry, 66*(44), 11748-11756. http://doi.org/**10.1021/acs.jafc.8b04000**.

Gao, H., Xu, J., Tan, M., Mu, D., Li, X., Zhao, Y., & Zheng, Z. (2021). Effect of high-intensity ultrasound soymilk pretreatment on the physicochemical properties of microbial transglutaminase-catalyzed tofu gel. *Journal of food science, 86*(6), 2410-2420. http://doi.org/**10.1111/1750-3841.15735**.

Ghosh, A., Ali, M. A., & Dias, G. J. (2009). Effect of cross-linking on microstructure and physical performance of casein protein. *Biomacromolecules, 10*(7), 1681-1688. http://doi.org/**10.1021/bm801341x**.

Gueguen, J., Chevalier, M., And, J. B., & Schaeffer, F. (1988). Dissociation and aggregation of pea legumin induced by pH and ionic strength. *Journal of the Science of Food and Agriculture, 44*(2), 167-182. http://doi.org/10.1002/jsfa.2740440208.

Holt, C., & Sawyer, L. (1993). Caseins as rheomorphic proteins: interpretation of primary and secondary structures of the α S1-, β-and κ-caseins. *Journal of the Chemical Society, Faraday Transactions, 89*(15), 2683-2692. http://doi.org/10.1039/FT9938902683.

Huppertz, T., Fox, P., & Kelly, A. (2018). The caseins: Structure, stability, and functionality. In *Proteins in food processing* (pp. 49-92): Elsevier. http://doi.org/10.1016/B978-0-08-100722-8.00004-8.

Khalesi, H., Sun, C., He, J., Lu, W., & Fang, Y. (2021). The role of amyloid fibrils in the modification of whey protein isolate gels with the form of stranded and particulate microstructures. *Food Research International, 140*, 109856. http://doi.org/10.1016/j.foodres.2020.109856.

Kornet, R., Shek, C., Venema, P., van der Goot, A. J., Meinders, M., & van der Linden, E. (2021). Substitution of whey protein by pea protein is facilitated by specific fractionation routes. *Food hydrocolloids, 117*, 106691. http://doi.org/10.1016/j.foodhyd.2021.106691.

Ladjal-Ettoumi, Y., Boudries, H., Chibane, M., & Romero, A. (2016). Pea, chickpea and lentil protein isolates: Physicochemical characterization and emulsifying properties. *Food Biophysics, 11*(1), 43-51. http://doi.org/10.1007/s11483-015-9411-6.

Larre, C., Chiarello, M., Dudek, S., Chenu, M., & Gueguen, J. (1993). Action of transglutaminase on the constitutive polypeptides of pea legumin. *Journal of agricultural and food chemistry, 41*(11), 1816-1820. http://doi.org/10.1021/jf00035a002.

Larre, C., Kedzior, Z. M., Chenu, M. G., Viroben, G., & Gueguen, J. (1992). Action of transglutaminase on an 11 S seed protein (pea legumin): influence of the substrate conformation. *Journal of agricultural and food chemistry, 40*(7), 1121-1126. http://doi.org/10.1021/jf00019a006.

Li, Guo, C., Yang, X., & Guo, Y. (2022). Acid-induced mixed methylcellulose and casein gels: Structures, physical properties and formation mechanism. *Food Chemistry, 366*, 130561. http://doi.org/10.1016/j.foodchem.2021.130561.

Li, H., Yang, C., Chen, C., Ren, F., Li, Y., Mu, Z., & Wang, P. (2018). The use of trisodium citrate to improve the textural properties of acid-Induced, transglutaminase-treated micellar casein gels. *Molecules, 23*(7), 1632. http://doi.org/10.3390/molecules23071632.

Lin, D., Zhang, L., Li, R., Zheng, B., Rea, M. C., & Miao, S. (2019). Effect of plant protein mixtures on the microstructure and rheological properties of myofibrillar protein gel derived from red sea bream (Pagrosomus major). *Food hydrocolloids, 96*, 537-545. http://doi.org/10.1016/j.foodhyd.2019.05.043.

Liu, Y., Zhang, Y., Guo, Z., Wang, C., Kang, H., Li, J., Wang, W., Li, Y., Lu, F., & Liu, Y. (2020). Enhancing the functional characteristics of soy protein isolate via cross-linking catalyzed by Bacillus subtilis transglutaminase. *J Sci Food Agric*. http://doi.org/10.1002/jsfa.11052.

Ma, Z., Li, L., Wu, C., Huang, Y., Teng, F., & Li, Y. (2022). Effects of combined enzymatic and ultrasonic treatments on the structure and gel properties of soybean protein isolate. *LWT, 158*, 113123. http://doi.org/10.1016/j.lwt.2022.113123.

McClements, D. J., & Grossmann, L. (2021). A brief review of the science behind the design of healthy and sustainable plant-based foods. *NPJ science of food, 5*(1), 1-10. http://doi.org/10.1038/s41538-021-00099-y.

Mession, J.-L., Roustel, S., & Saurel, R. (2017). Interactions in casein micelle – Pea protein system (part I): Heat-induced denaturation and aggregation. *Food hydrocolloids, 67*, 229-242. http://doi.org/10.1016/j.foodhyd.2015.12.015.

Moure, A., Sineiro, J., Domínguez, H., & Parajó, J. C. (2006). Functionality of oilseed protein products: A review. *Food Research International, 39*(9), 945-963. http://doi.org/10.1016/j.foodres.2006.07.002.

Nicolai, T., & Chassenieux, C. (2021). Heat-induced gelation of casein micelles. *Food hydrocolloids, 118*, 106755. http://doi.org/10.1016/j.foodhyd.2021.106755.

O'connell, J., & Fox, P. (2003). Heat-induced coagulation of milk. In *Advanced Dairy Chemistry—1 Proteins* (pp. 879-945). Boston, MA.: Springer. http://doi.org/10.1007/978-1-4419-8602-3_25.

Peng, X., & Guo, S. (2015). Texture characteristics of soymilk gels formed by lactic fermentation: A comparison of soymilk prepared by blanching soybeans under different temperatures. *Food hydrocolloids, 43*, 58-65. http://doi.org/**10.1016/j.foodhyd.2014.04.034**.

Pereira, R., Bennett, R., Hemar, Y., & Campanella, O. (2001). Rheological and microstructural characteristics of model processed cheese analogues. *Journal of Texture Studies, 32*(5-6), 349-373. http://doi.org/10.1111/j.1745-4603.2001.tb01242.x.

Qin, X. S., Luo, S. Z., Cai, J., Zhong, X. Y., Jiang, S. T., Zhao, Y. Y., & Zheng, Z. (2016). Transglutaminase-induced gelation properties of soy protein isolate and wheat gluten mixtures with high intensity ultrasonic pretreatment. *Ultrason Sonochem, 31*, 590-597. http://doi.org/10.1016/j.ultsonch.2016.02.010.

Raak, N., & Corredig, M. (2022). Kinetic aspects of casein micelle cross-linking by transglutaminase at different volume fractions. *Food hydrocolloids, 128*, 107603. http://doi.org/10.1016/j.foodhyd.2022.107603.

Raikos, V., Campbell, L., & Euston, S. R. (2007). Rheology and texture of hen's egg protein heat-set gels as affected by pH and the addition of sugar and/or salt. *Food hydrocolloids, 21*(2), 237-244. http://doi.org/10.1016/j.foodhyd.2006.03.015.

Shevkani, K., & Chourasia, S. (2021). Dietary Proteins: Functions, Health Benefits and Healthy Aging. In *Nutrition, Food and Diet in Ageing and Longevity* (pp. 3-37): Springer. http://doi.org/10.1007/978-3-030-83017-5_1.

Steinfeld, B., Scott, J., Vilander, G., Marx, L., Quirk, M., Lindberg, J., & Koerner, K. (2015). The role of lean process improvement in implementation of evidence-based practices in behavioral health care. *The Journal of Behavioral Health Services & Research, 42*(4), 504-518. http://doi.org/**10.1007/s11414-013-9386-3**.

Sun, X. D., & Arntfield, S. D. (2012). Molecular forces involved in heat-induced pea protein gelation: Effects of various reagents on the rheological properties of salt-extracted pea protein gels. *Food hydrocolloids, 28*(2), 325-332. http://doi.org/10.1016/j.foodhyd.2011.12.014.

Tang, C. H., Wu, H., Yu, H. P., Li, L., Chen, Z., & Yang, X. Q. (2006). Coagulation and gelation of soy protein isolates induced by microbial transglutaminase. *Journal of Food Biochemistry, 30*(1), 35-55. http://doi.org/10.1111/j.1745-4514.2005.00049.x.

Tang, Q., Roos, Y. H., & Miao, S. (2023). Plant Protein versus Dairy Proteins: A pH-Dependency Investigation on Their Structure and Functional Properties. *Foods, 12*(2), 368. http://doi.org/10.3390/foods12020368.

559 Wu, C., Wang, J., Yan, X., Ma, W., Wu, D., & Du, M. (2020). Effect of partial replacement of
560 water-soluble cod proteins by soy proteins on the heat-induced aggregation and
561 gelation properties of mixed protein systems. *Food hydrocolloids, 100*, 105417.
562 http://doi.org/**10.1016/j.foodhyd.2019.105417**.
563 Yang, Ren, Y., Liu, H., Huo, C., & Li, L. (2021). Differences in the physicochemical, digestion and
564 microstructural characteristics of soy protein gel acidified with lactic acid bacteria,
565 glucono-δ-lactone and organic acid. *International Journal of Biological*
566 *Macromolecules, 185*, 462-470. http://doi.org/**10.1016/j.ijbiomac.2021.06.071**.
567 Yuan, C., Xu, D., Cui, B., & Wang, Y. (2019). Gelation of κ-carrageenan/Konjac glucommanan
568 compound gel: Effect of cyclodextrins. *Food hydrocolloids, 87*, 158-164.
569 http://doi.org/10.1016/j.foodhyd.2018.07.037.
570 Zha, F., Rao, J., & Chen, B. (2021). Modification of pulse proteins for improved functionality
571 and flavor profile: A comprehensive review. *Comprehensive Reviews in Food Science*
572 *and Food Safety, 20*(3), 3036-3060. http://doi.org/**10.1111/1541-4337.12736**.
573 Zheng, L., Regenstein, J. M., Zhou, L., & Wang, Z. (2022). Soy protein isolates: A review of their
574 composition, aggregation, and gelation. *Comprehensive Reviews in Food Science and*
575 *Food Safety, 21*(2), 1940-1957. http://doi.org/10.1111/1541-4337.12925.
576 Zhou, X., Zheng, Y., Zhong, Y., Wang, D., & Deng, Y. (2022). Casein-hempseed protein complex
577 via cross-link catalyzed by transglutaminase for improving structural, rheological,
578 emulsifying and gelation properties. *Food Chemistry, 383*, 132366.
579 http://doi.org/**10.1016/j.foodchem.2022.132366**.
580 Zhu, P., Huang, W., Guo, X., & Chen, L. (2021). Strong and elastic pea protein hydrogels formed
581 through pH-shifting method. *Food hydrocolloids, 117*.
582 http://doi.org/10.1016/j.foodhyd.2021.106705.

583

584

585

586

587

588

589

590

591

592 **Table 1.** Rheological parameters (temperature sweep) of heat-induced SPI, LPI and
593 WPI gels as a function of pH.

| Samples | Temperature sweep | | |
|---|---|---|---|
| | G′ (Pa) | G″ (Pa) | Tan δ |
| SPI-3 | 568 ± 155$^{a}$ | 130 ± 34 $^{ab}$ | 0.23 ± 0.00$^{e}$ |
| LPI-3 | 5366 ± 110$^{c}$ | 558 ± 37$^{b}$ | 0.10 ± 0.00$^{a}$ |
| WPI-3 | 4965 ± 255$^{c}$ | 559 ± 33$^{b}$ | 0.11 ± 0.00$^{a}$ |
| SPI-5 | 177 ± 62 $^{a}$ | 36 ± 2$^{a}$ | 0.22 ± 0.07$^{de}$ |
| LPI-5 | 313 ± 112$^{a}$ | 54 ± 7$^{a}$ | 0.18 ± 0.04$^{cde}$ |
| WPI-5 | 7295 ± 502$^{d}$ | 1296 ± 136$^{c}$ | 0.18 ± 0.01$^{bcd}$ |
| SPI-7 | 692 ± 128$^{a}$ | 87 ± 13$^{a}$ | 0.13 ± 0.00$^{ab}$ |
| LPI-7 | 2026 ± 484$^{b}$ | 294 ± 88$^{ab}$ | 0.14 ± 0.01$^{abc}$ |
| WPI-7 | 26272 ± 846$^{f}$ | 3086 ± 631$^{d}$ | 0.12 ± 0.02$^{a}$ |
| SPI-9 | 946 ± 37$^{a}$ | 117 ± 4$^{ab}$ | 0.12 ± 0.00$^{a}$ |
| LPI-9 | 47 ± 15$^{a}$ | 48 ± 15$^{a}$ | 1.01 ± 0.01$^{f}$ |
| WPI-9 | 16115 ± 629$^{e}$ | 1458 ± 57$^{c}$ | 0.09 ± 0.00$^{a}$ |

594 Names of samples with numbers indicate the protein isolate gels obtained at the
595 corresponding pH conditions. Significant different ($p \leq 0.05$) among protein gels was
596 denoted by different letters.

597

598

599

600

**Table 2.** Power-law parameters (frequency sweep) of heat-induced SPI, LPI and WPI gels as a function of pH.

| Samples | K′ (Pa· $s^n$) | n′ | $R^2$ Eq. (1) | K″ (Pa· $s^n$) | n″ | $R^2$ Eq. (2) |
|---|---|---|---|---|---|---|
| SPI-3 | 480 ± 137$^{a}$ | 0.060 ± 0.004$^{a}$ | 0.9347 | 92 ± 36$^{a}$ | 0.132 ± 0.004$^{de}$ | 0.9741 |
| LPI-3 | 4942 ± 140$^{c}$ | 0.058 ± 0.001$^{a}$ | 0.9959 | 492 ± 77$^{c}$ | 0.086 ± 0.020$^{abc}$ | 0.9370 |
| WPI-3 | 4485 ± 173$^{c}$ | 0.068 ± 0.001$^{ab}$ | 0.9948 | 498 ± 40$^{c}$ | 0.083 ± 0.010$^{ab}$ | 0.9838 |
| SPI-5 | 150 ± 59$^{a}$ | 0.094 ± 0.030$^{c}$ | 0.9821 | 28 ± 3$^{a}$ | 0.153 ± 0.024$^{e}$ | 0.9968 |
| LPI-5 | 236 ± 44$^{a}$ | 0.070 ± 0.003$^{ab}$ | 0.9639 | 45 ± 9$^{a}$ | 0.130 ± 0.003$^{de}$ | 0.9683 |
| WPI-5 | 6362 ± 480$^{d}$ | 0.095 ± 0.002$^{c}$ | 0.9954 | 1040 ± 83$^{d}$ | 0.108 ± 0.012$^{bcd}$ | 0.9411 |
| SPI-7 | 617 ± 120$^{a}$ | 0.076 ± 0.000$^{abc}$ | 0.9834 | 77 ± 16$^{a}$ | 0.094 ± 0.012$^{abc}$ | 0.9240 |
| LPI-7 | 1773 ± 438$^{b}$ | 0.086 ± 0.007$^{bc}$ | 0.9985 | 241 ± 82$^{b}$ | 0.112 ± 0.006$^{cd}$ | 0.9860 |
| WPI-7 | 24128 ± 882$^{f}$ | 0.062 ± 0.001$^{a}$ | 0.9981 | 2434 ± 89$^{f}$ | 0.070 ± 0.004$^{a}$ | 0.9267 |
| SPI-9 | 841 ± 34$^{a}$ | 0.070 ± 0.002$^{ab}$ | 0.9929 | 100 ± 5$^{a}$ | 0.094 ± 0.010$^{abc}$ | 0.9676 |
| LPI-9 | 65 ± 10$^{a}$ | 0.177 ± 0.013$^{d}$ | 0.9962 | 69 ± 4$^{a}$ | 0.123 ± 0.007$^{d}$ | 0.9946 |
| WPI-9 | 14821 ± 91$^{e}$ | 0.058 ± 0.002$^{a}$ | 0.9855 | 1340 ± 8$^{e}$ | 0.076 ± 0.002$^{a}$ | 0.9888 |

Names of samples with numbers indicate the protein isolate gels obtained at the corresponding pH conditions. Significant different ($p \leq 0.05$) among protein gels was denoted by different letters.

606 **Table 3.** Mechanical properties and water holding capacity (WHC) of thermal-induced
607 SPI, LPI, and WPI gels as a function of pH.

| Samples | Hardness (g) | Springiness (%) | WHC (%) |
|---|---|---|---|
| SPI-3 | $125.95 \pm 30.08^{a}$ | $62.66 \pm 1.64^{a}$ | $64.96 \pm 4.04^{a}$ |
| LPI-3 | $606.48 \pm 2.16^{d}$ | $90.66 \pm 1.44^{e}$ | $91.17 \pm 0.47^{ef}$ |
| WPI-3 | $545.95 \pm 14.46^{d}$ | $93.79 \pm 3.38^{ef}$ | $92.84 \pm 0.40^{fg}$ |
| WPI-5 | $622.05 \pm 30.14^{d}$ | $92.69 \pm 0.62^{ef}$ | $87.71 \pm 2.55^{e}$ |
| SPI-7 | $251.82 \pm 55.27^{ab}$ | $70.33 \pm 1.70^{b}$ | $73.04 \pm 0.68^{b}$ |
| LPI-7 | $461.78 \pm 4.89^{cd}$ | $83.66 \pm 1.13^{d}$ | $82.99 \pm 0.81^{d}$ |
| WPI-7 | $1930.95 \pm 79.33^{f}$ | $96.89 \pm 2.71^{f}$ | $98.73 \pm 0.45^{h}$ |
| SPI-9 | $319.56 \pm 14.24^{bc}$ | $76.55 \pm 1.77^{c}$ | $77.12 \pm 1.33^{c}$ |
| WPI-9 | $1202.44 \pm 205.84^{e}$ | $94.14 \pm 1.44^{ef}$ | $96.27 \pm 0.96^{gh}$ |

608 Names of samples with numbers indicate the protein isolate gels obtained at the
609 corresponding pH conditions. Significant different ($p \leq 0.05$) among protein gels was
610 denoted by different letters.

611

612

613

614

615

616

617

618

**Table 4.** FTIR analysis of thermal-induced SPI, LPI, and WPI gels as a function of pH.

| Samples | α-helix | Intramolecular β-sheet | Aggregated β-sheet | β-turn | Random coil | Side chain |
|---|---|---|---|---|---|---|
| SPI-3 | 21.73 ± 1.00$^{bcd}$ | 19.15 ± 0.25$^{ab}$ | 15.15 ± 0.87$^{b}$ | 11.09 ± 1.82$^{bc}$ | 32.78 ± 0.35$^{ef}$ | 0.11 ± 0.05$^{a}$ |
| LPI-3 | 19.83 ± 1.32$^{abc}$ | 22.08 ± 0.27$^{bcd}$ | 14.47 ± 0.30$^{ab}$ | 9.36 ± 1.37$^{abc}$ | 34.05 ± 0.80$^{f}$ | 0.05 ± 0.03$^{a}$ |
| WPI-3 | 16.78 ± 2.13$^{a}$ | 24.37 ± 0.17$^{de}$ | 12.05 ± 1.56$^{a}$ | 8.16 ± 0.64$^{ab}$ | 38.58 ± 3.22$^{g}$ | 0.04 ± 0.03$^{a}$ |
| SPI-5 | 19.34 ± 1.36$^{ab}$ | 21.25 ± 0.29$^{abcd}$ | 16.23 ± 0.32$^{bc}$ | 11.13 ± 2.65$^{bc}$ | 32.00 ± 3.44$^{ef}$ | 0.05 ± 0.04$^{a}$ |
| LPI-5 | 21.82 ± 0.90$^{bcd}$ | 23.68 ± 0.18$^{cde}$ | 18.03 ± 0.42$^{cd}$ | 11.86 ± 0.78$^{c}$ | 24.54 ± 0.34$^{bc}$ | 0.07 ± 0.02$^{a}$ |
| WPI-5 | 18.93 ± 0.87$^{ab}$ | 26.47 ± 2.71$^{e}$ | 18.47 ± 2.60$^{cd}$ | 5.91 ± 0.05$^{a}$ | 30.16 ± 0.84$^{def}$ | 0.07 ± 0.02$^{a}$ |
| SPI-7 | 26.55 ± 0.40$^{ef}$ | 20.55 ± 2.26$^{abc}$ | 18.95 ± 0.86$^{cde}$ | 8.43 ± 0.76$^{abc}$ | 25.46 ± 1.78$^{bcd}$ | 0.05 ± 0.01$^{a}$ |
| LPI-7 | 23.61 ± 1.07$^{cde}$ | 18.19 ± 0.96$^{a}$ | 20.55 ± 0.93$^{def}$ | 9.17 ± 2.97$^{abc}$ | 28.38 ± 1.88$^{cde}$ | 0.11 ± 0.04$^{a}$ |
| WPI-7 | 29.20 ± 0.11$^{fg}$ | 19.67 ± 0.34$^{ab}$ | 22.07 ± 0.23$^{f}$ | 6.68 ± 0.09$^{a}$ | 22.26 ± 0.16$^{b}$ | 0.11 ± 0.03$^{a}$ |
| SPI-9 | 30.99 ± 3.67$^{g}$ | 24.24 ± 0.69$^{de}$ | 19.42 ± 1.90$^{def}$ | 7.94 ± 0.59$^{ab}$ | 17.34 ± 1.65$^{a}$ | 0.07 ± 0.03$^{a}$ |
| LPI-9 | 26.30 ± 2.63$^{ef}$ | 17.81 ± 2.18$^{a}$ | 21.52 ± 0.92$^{ef}$ | 7.10 ± 0.12$^{a}$ | 26.93 ± 3.66$^{bcd}$ | 0.33 ± 0.12$^{b}$ |
| WPI-9 | 25.00 ± 1.84$^{de}$ | 20.41 ± 2.70$^{abc}$ | 19.45 ± 0.65$^{def}$ | 8.76 ± 1.89$^{abc}$ | 26.36 ± 2.00$^{bcd}$ | 0.02 ± 0.02$^{a}$ |

Names of samples with numbers indicate the protein isolate gels obtained at the corresponding pH conditions. Significant different ($p \leq 0.05$) among protein gels was denoted by different letters.

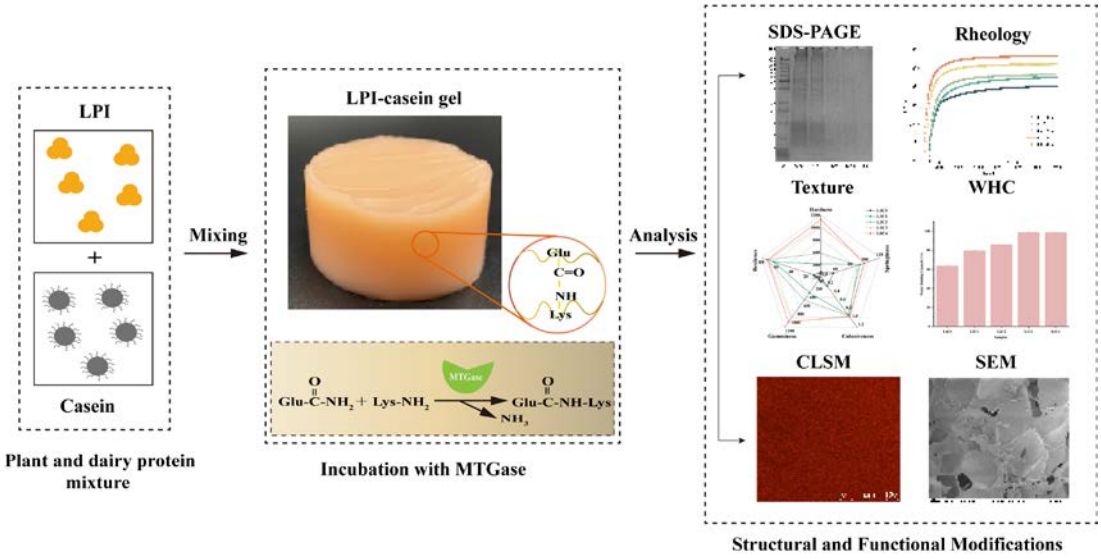


624

625 **Graphical abstract**

626

627

628

629

630

631

632

633

634

635

**Fig. 1.** Appearance of LPI/casein mixtures (a) without MTGase and gels (b) with MTGase at 50 ℃. L4C0, L3C1, L2C2, L1C3, L0C4 refers the mixture of the LPI: Casein ratio of 4:0, 3:1, 2:2, 1:3, 0:4, respectively.

**Fig. 2.** SDS-PAGE patterns of LPI/casein mixtures and gels with/without MTGase treatment at 50 ℃. M: marker. (a) and (b) mean LPI/casein mixtures without MTGase treatment under NR and R conditions, respectively. (c) and (d) mean LPI/casein gels with MTGase treatment under NR and R conditions, respectively. L4C0, L3C1, L2C2, L1C3, L0C4 refer the MTGase-induced gels prepared with the LPI: Casein ratio of 4:0, 3:1, 2:2, 1:3, 0:4, respectively.

**Fig. 3.** Time sweep (a-b) and frequency sweep (c-d) of LPI/casein gels induced by MTGase. G' and G″ means storage modulus and loss modulus of gels, respectively. L4C0, L3C1, L2C2, L1C3, L0C4 refer the MTGase-induced gels prepared with the LPI: Casein ratio of 4:0, 3:1, 2:2, 1:3, 0:4, respectively.

**Fig. 4.** Visual appearance (a-e), CLSM (f-j) and SEM images (k-o) of the mixed LPI/casein gels. Scale bars = 100 μm for CLSM and SEM images. L4C0, L3C1, L2C2, L1C3, L0C4 refer the MTGase-induced gels prepared with the LPI: Casein ratio of 4:0, 3:1, 2:2, 1:3, 0:4, respectively.

**Fig. 1.**

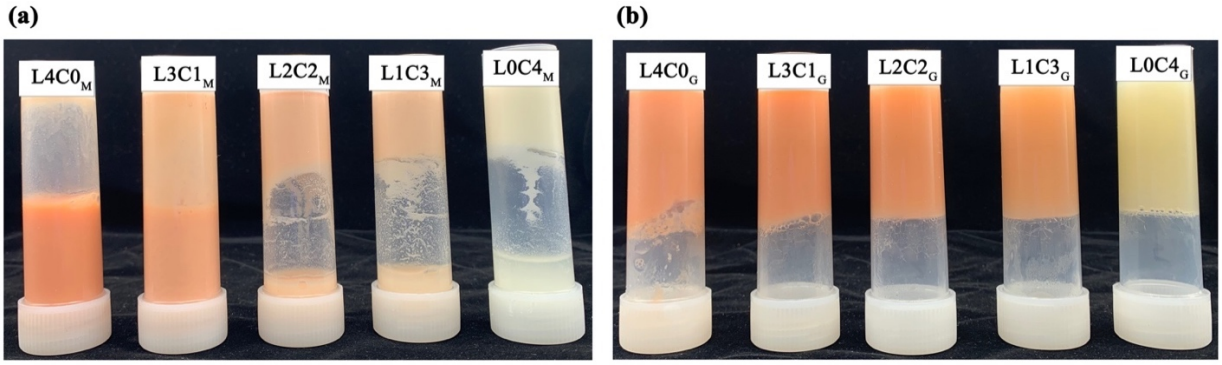
(a)
L4C0M
L3C1M
L2C2M
L1C3M
L0C4M
(b)
L4C0G
L3C1G
L2C2G
L1C3G
L0C4G

672 **Fig. 2.**

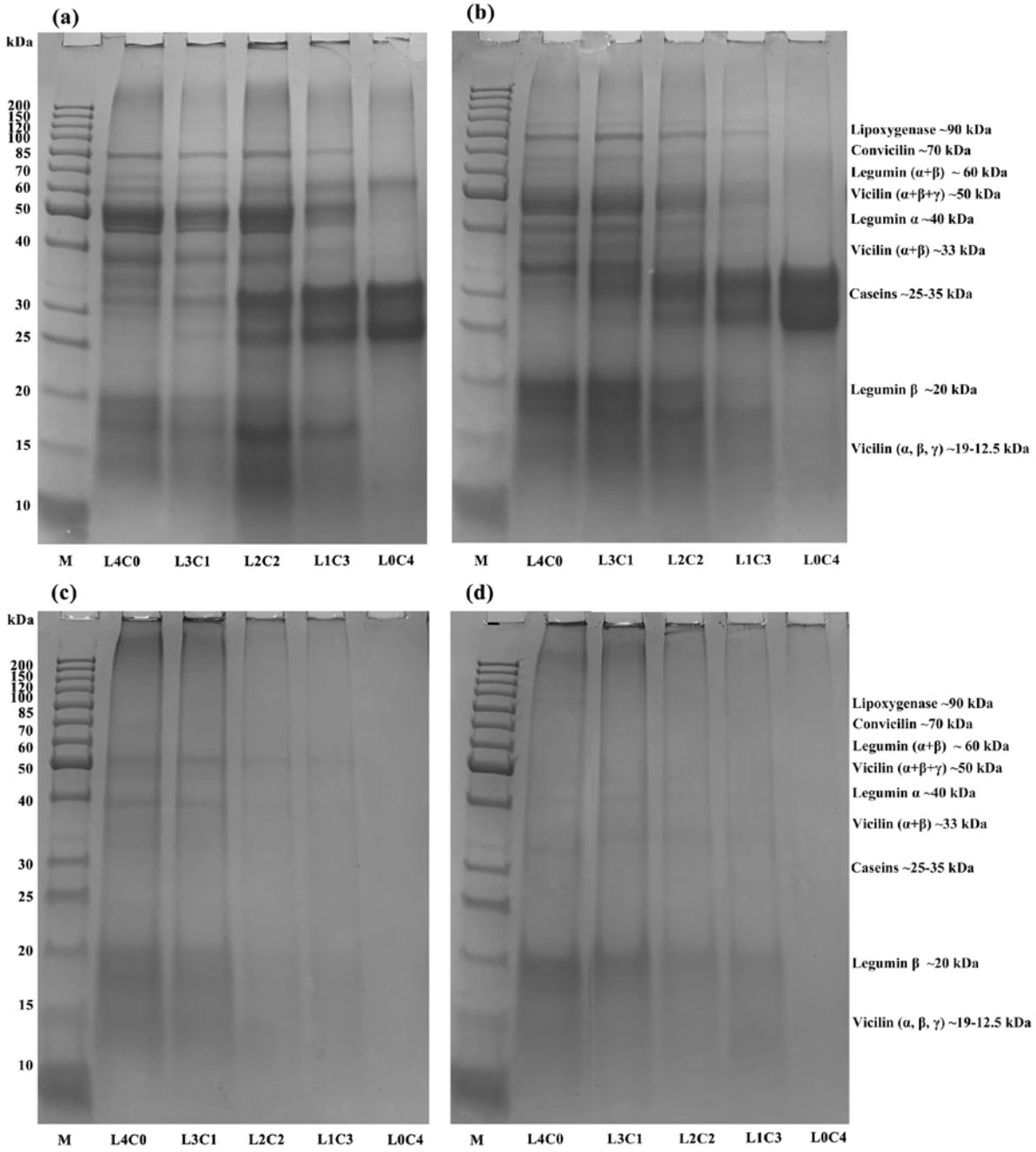


673

674

675

676

677 **Fig. 3.**

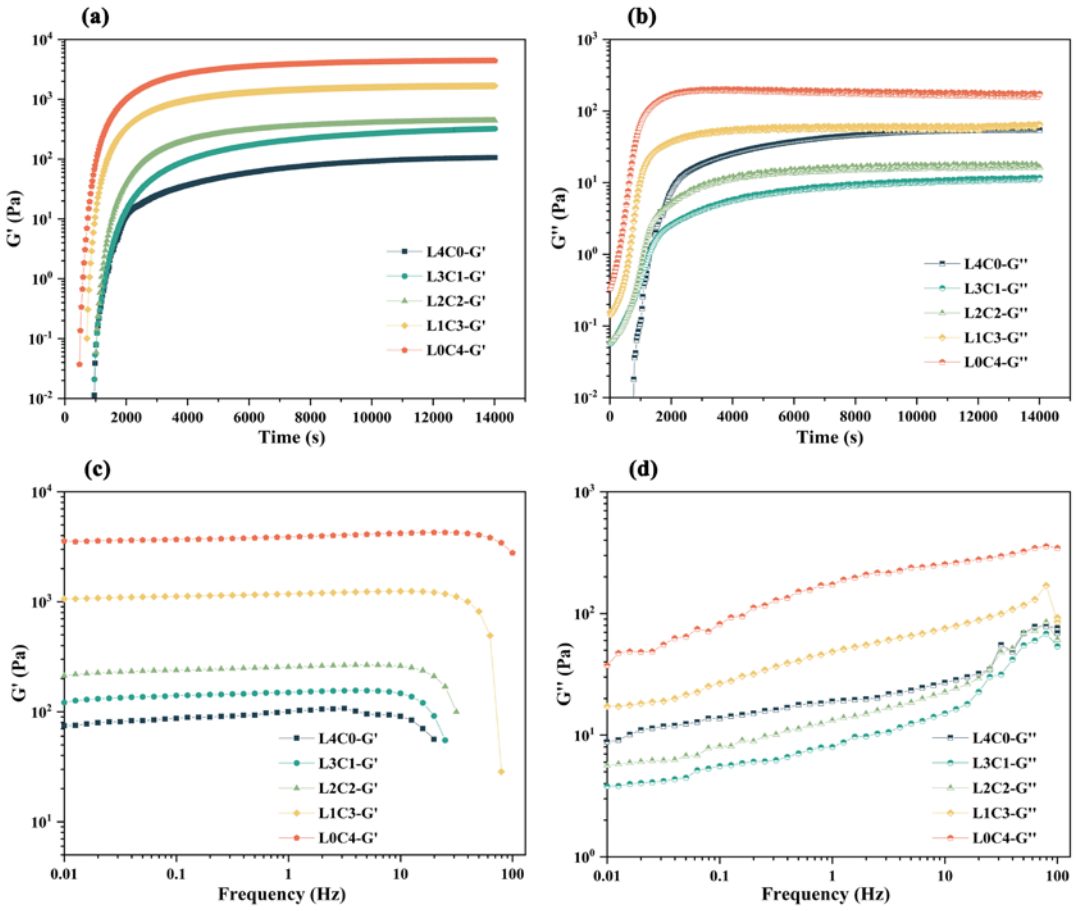


678

679

680

681

682

683

684

685

686

687

688

689

**Fig. 4.**

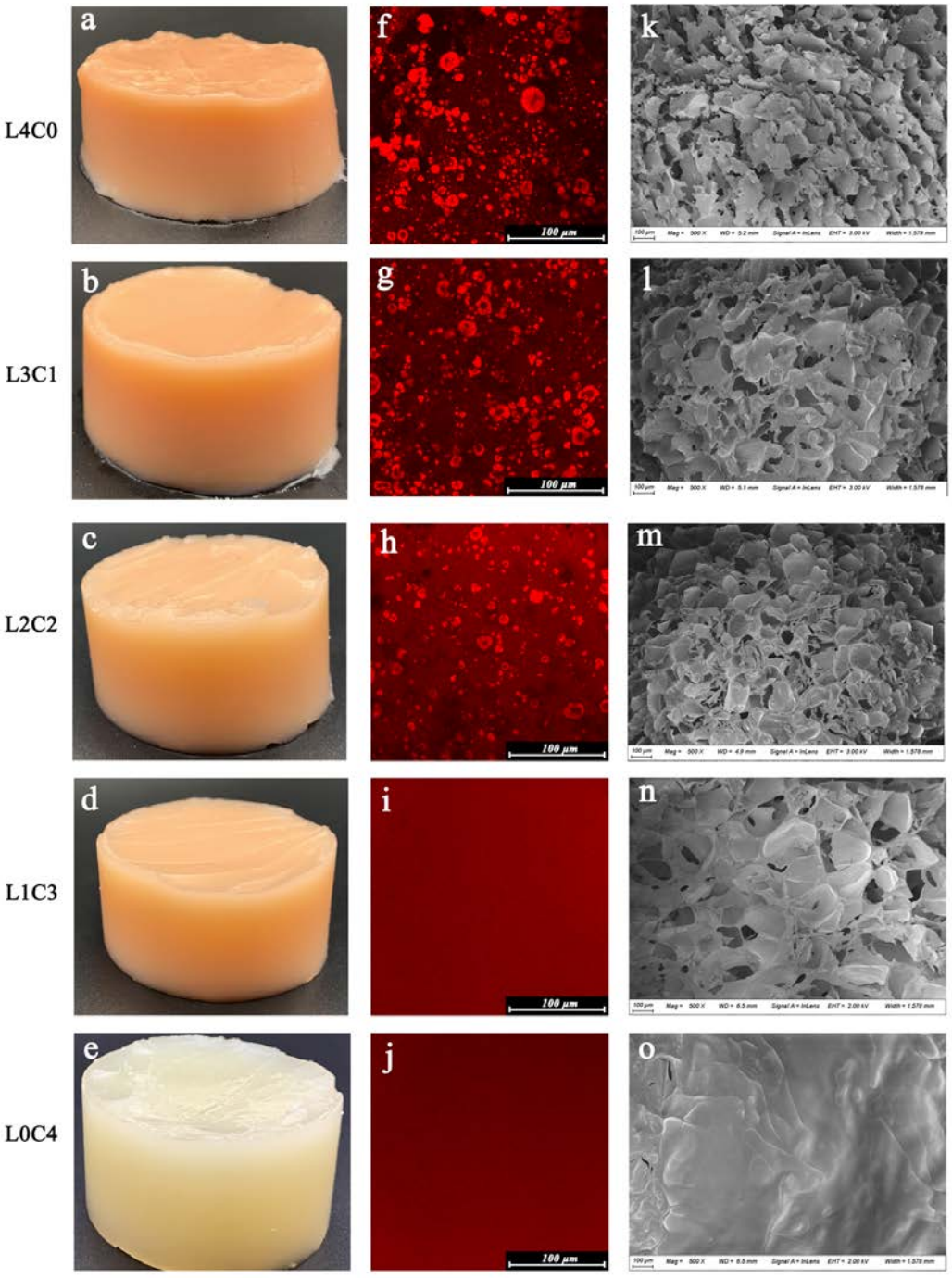


690